Geomorphology 228 (2015) 504–511

Contents lists available at ScienceDirect

Geomorphology

journal homepage: www.elsevier.com/locate/geomorph

The role of windstorm exposure and yellow cedar decline on landslide susceptibility in southeast Alaskan temperate rainforests

Brian Buma *, Adelaide C. Johnson

Dept. of Natural Sciences, University of Alaska Southeast, 11120 Glacier Hwy, Juneau, AK 99801, USA

ARTICLE INFO

Article history:
Received 31 May 2014
Received in revised form 8 October 2014
Accepted 14 October 2014
Available online xxxx

Keywords:
Multiple disturbances
Disturbance interactions
Landslide
Windstorm
Temperate perhumid rainforest
Yellow cedar decline

ABSTRACT

Interactions between ecological disturbances have the potential to alter other disturbances and their associated regimes, such as the likelihood, severity, and extent of events. The influence of exposure to wind and yellow cedar decline on the landslide regime of Alaskan temperate rainforests was explored using presence-only modeling techniques. The wind regime was found to be a significant influence on the spatial distribution of landslide events. This effect was mediated by slope, with little interactive effects at low angles and stronger influences on steeper slopes. Mechanistically, the interaction appears to be mediated by root strength, which is an important factor in stability of high-angle slopes. Yellow cedar decline, despite increasing landslide susceptibility in fine-scale studies, was not significant—although a stronger relationship may develop with time. Overall, inclusion of other disturbances in the modeling framework resulted in a significant spatial refinement when predicting landslide susceptibility. This results from the varying importance of individual disturbance drivers across the landscape, of which only a subset are exposed to potential disturbance interactions. This spatial effect is an important consideration when characterizing landscape-scale disturbance regimes and their interactions with other disturbances.

1. Introduction

Natural disturbances such as windthrow, fires, landslides, and insect outbreaks play a large role in forest ecosystem structure and functioning (White, 1979; Turner, 2010; Edburg et al., 2012). These events regulate broad landscape-scale processes such as biomass dynamics (Kashian et al., 2006), nutrient cycling (McLauchlan et al., 2014), and species diversity. Although individual disturbances and their associated regimes have been important study topics for several decades, interactions between multiple disturbances are also of crucial interest in the field of landscape ecology because of their potential to create nonlinear and often unexpected synergistic outcomes (Paine et al., 1998; Turner, 2010), such as altered disturbance likelihoods (Kulakowski et al., 2003), severities (Kulakowski and Veblen, 2007), and recovery trajectories (Buma and Wessman, 2011). Disturbance interactions can also shape the spatial characteristics of regional disturbance regimes. For example, Veblen et al. (1994) focused on the coarse-scale spatial patterning of multiple events (fire, avalanche, and insect mortality) via forest history reconstructions. Among the disturbance regime interactions they describe, avalanches play a fundamental role in limiting fire size, thus altering the spatial patterning (location and extent) of the fire regime in those landscapes. A better understanding of those disturbances/interactions is necessary given the expected changes to disturbance regimes in the future (Dale et al., 2001) and the potential for rapid changes associated with changing disturbance regimes (Paine et al., 1998; Buma et al., 2013).

Detailed investigations of disturbance interactions are typically achieved at fine scales, usually on single events or small groups of events (e.g., fire and wind: Buma and Wessman, 2011; landslides and yellow cedar decline: Johnson and Wilcock, 2002). These mechanistic studies of interaction processes are vital, yet scaling from single events to regional disturbance regimes remains difficult owing to a variety of contingent factors, spatial autocorrelation, and other confounding factors that make mechanistic relationships unclear at coarse scales (Wiens and Parker, 1995; Parker and Wiens, 2005). Interaction mechanisms important at fine scales are not always certain to be significant at coarser scales of analysis (their generality) or if the effects are constant across landscapes (their homogeneity); these linkages remain a challenge temporally (Buma, 2014) and spatially (Johnson and Cochrane, 2003; Turner, 2010).

Perhumid rainforests provide an excellent opportunity for studying the interaction of disturbance regimes because of their relative simplicity (in terms of disturbances). The primary, large natural disturbances are wind, avalanches, and landslides (Alaback, 1991; Veblen and Alaback, 1996) and have been well-examined in intensive, plot-scale

* Corresponding author. Tel.: +1 907 796 6410.
E-mail address: brian.buma@uas.alaska.edu (B. Buma).

http://dx.doi.org/10.1016/j.geomorph.2014.10.014
0169-555X/

studies. Climatic variability is low (Alaback, 1991), anthropogenic presence minimal, and forest tree species diversity low and relatively consistent (DellaSala et al., 2011), reducing variance across the landscape. Therefore, the interaction between disturbance regimes at landscape scales is more easily isolated relative to the influence of species composition or climate.

Wind is a major forest disturbance globally (Walter, 1984; Mitchell, 2013); in the perhumid rainforests of the Pacific Northwest coast of North America, wind is the principal forest disturbance (Nowaki and Kramer, 1998; Alaback et al., 2013). At one estimate, wind was responsible for ~25% of all observed mortality in monitored stands over a 7-year period in the region (southeast Alaska; Hutchinson and LaBau, 1975), and it has been estimated that 15–33% of productive forest in southeast Alaska is exposed to major wind disturbances (Alaback et al., 2013). The wind disturbance regime is dominated by winter season, southerly storms (southeast to southwest; Harris, 1999). These disturbances span a range of intensities and extents, from large, 100+ ha events to small, <1 ha patches (Nowaki and Kramer, 1998). Landscapes subject to this wind disturbance regime are often younger, denser, and more productive than more protected locations (Kramer et al., 2001; Alaback et al., 2013) and provide important habitat for species such as black bear, *Ursus americanus* (DeGayner et al., 2005).

Landslides are also important high severity events, which occur at a variety of scales from large, rare events to small, but chronic slide locations (Veblen and Alaback, 1996), principally related to topography (Swanston, 1997). Generally, slide events in temperate rainforests of Alaska are of the debris-avalanche–debris-flow sequence type (Varnes, 1978; Sidle et al., 1985; Hungr et al., 2001). These landslides result from altered surface loading, increased soil water levels, removal of mechanical support (e.g., tree roots), or a combination of those factors (Terzaghi, 1943; Swanston, 1974; Sidle, 1992). In southeast Alaska these failures typically are rapid in shallow soils (<2 m.) and on high angle (>30°) slopes (Johnson et al., 2000); slow moving, deep seated earthflows are very rare because of the general steep slopes, shallow soils, and heavy rainfall (D. Landwehr, USFS, *personal communication*, 2014). Landslides typically occur in depressions in hillslopes, where soil and moisture accumulate and subsequently fail cyclically on a 300–500+ year return interval (Montgomery and Deitrich, 1994; Swanston, 1997).

The slope stability model (simplified version of the infinite slope model, expressed in Eq. (1) as the Factor of Safety (FS); Swanston, 1997) is appropriate for the wide, shallow slides of the debris-avalanche –debris-flow sequence and is often used to describe the interaction of predisposing components acting normal and parallel to potential slip surfaces (Wu and Sidle, 1995; Swanston, 1997).

$$FS = \frac{C + R + (\sigma - u)\ \tan\ \theta}{(Ws)Z + Wt + a} \qquad (1)$$

The FS model describes the ratio between forces resisting and forces promoting hillslope failure. Forces resisting failure include soil cohesion (C), root cohesion (R), and internal angle of soil friction ( ), as modified by normal stress (σ) and reduced with increasing pore pressure (u). Stability is reduced with increases in the loading parameters including soil depth (Z), weights of soil (W_s) and vegetation (W_t), and the downward force of wind acting on trees (a). As formulated and typically used, the FS model is deterministic (e.g., stable or instable), but it is used here as a conceptual model of factors promoting or resisting instability in a generalized landscape.

Conceptually, forest disturbance may alter the landslide regime by changing those factors governing hillslope stability via disrupting existing forest structural properties (Swanston, 1974; Wu et al., 1979; Johnson et al., 2000; Ammann et al., 2009; Pawlik, 2013). Tree roots can anchor into bedrock cracks and fractures (providing local stability) as well as network across hillslopes (providing additional strength laterally; Swanston, 1974). Removal of that root structure via tree mortality and subsequent decay result in weakened soil structures and the potential increased landslides (decreasing R). Wind may also affect slides by providing an additional downward force on standing trees attached to the soil (Wu et al., 1979).

Another emerging disturbance in the region is yellow cedar decline, the mass mortality of Alaskan yellow cedar (*Callitropsis nootkatensis*). Yellow cedar decline (YCD) has been linked to low snowpack and saturated soils, as cedar fine roots accumulate near the soil surface and are then susceptible to freezing mortality during cold events if not insulated by snow (Hennon et al., 2012). Similar to wind, YCD has the potential to modify the drivers of landslide initiation. Yellow cedar decline is associated with landslides via a reduction in root strength in shallow soils (<0.7 m), affecting R or changes in soil pore pressures in deeper soils (Johnson and Wilcock, 2002).

Generally, weight of the soil, vegetation, and slope have more influence than root strength (R; Swanston, 1997). Interactions between wind, YCD, and landslides are likely significant whenever factors promoting instability (high soil depths, steep slopes) are higher than frictional forces promoting stability, and soil cohesion and root strength are compensating. So the interaction effect is likely to be important primarily on steeper slopes, where a reduction in R or an increase in a would result in a significant change in slope stability. If that is the case, a spatial relationship should exist between slide occurrence and those factors which alter the FS equation.

The purpose of this study is to (i) determine if significant relationships exist between exposure to wind disturbance, the emerging disturbance of YCD, and landslide susceptibility at large spatial scales; and (ii) test if incorporating that interaction into susceptibility models improves model accuracy.

2. Study area and methods

The perhumid rainforest of the Pacific Northwest coast stretches >1000 km from British Columbia, Canada, to southeastern Alaska, USA (DellaSala et al., 2011). Kuiu Island in the Tongass National Forest (Fig. 1) was selected as the study area for two reasons. First, landslides have been mapped for the entire island (USFS, 2011), and second, a wind disturbance model was developed and tested on the island (Kramer et al., 2001; further details below). Kuiu is a large island (~2000 km^2) with a maximum elevation of 1039 m (Fig. 1). The island consists of steep terrain along the high-elevation crest with large, relatively low-lying, flat areas along the northeast portions. Precipitation, generally increasing with elevation, ranges from ~1500 to >5000 mm annually (SNAP, 2013; www.snap.uaf.edu). The dominant tree species are Sitka spruce (*Picea sitchensis*) and western and mountain hemlock (*Tsuga heterophylla* and *T. mertensiana*, respectively), with Alaskan yellow cedar and western redcedar (*Thuja plicata*) in lower concentrations. Shore pine (*Pinus contorta* var. *contorta*) is present in low-productivity bog sites. The geology consists primarily of plutonic mountains (26% of island area, 52% forested, 10% hydric bogs and wetlands), sedimentary hills (33% of island, 85% forested, 20% hydric), limestone ridges (6% of island, 83% forested, 18% hydric), and greywacke lowlands (61% of island, 59% forested, 49% hydric), as mapped by Kramer et al. (2001).

Landslides of the debris-avalanche–debris-flow type on Kuiu were mapped as part of a regional USFS mapping effort (USFS, 2011; Fig. 1, Table 1). Landslides were hand digitized from current imagery and dated if possible; failure type, vegetation cover, and other salient variables were estimated. Because this study focused on linkages between landslides, YCD, and wind in natural conditions, all landslides that were related to roads, logging activities, or occurring in nonvegetated areas (e.g., rockslides) were eliminated prior to analysis. Inside each slide, the highest elevation point was extracted and used as that slide's initiation point; the lowest as the end point. These restrictions left a total of 295 mapped landslides (Fig. 1, Table 1). All processing was conducted in R (R Core Team, 2013).

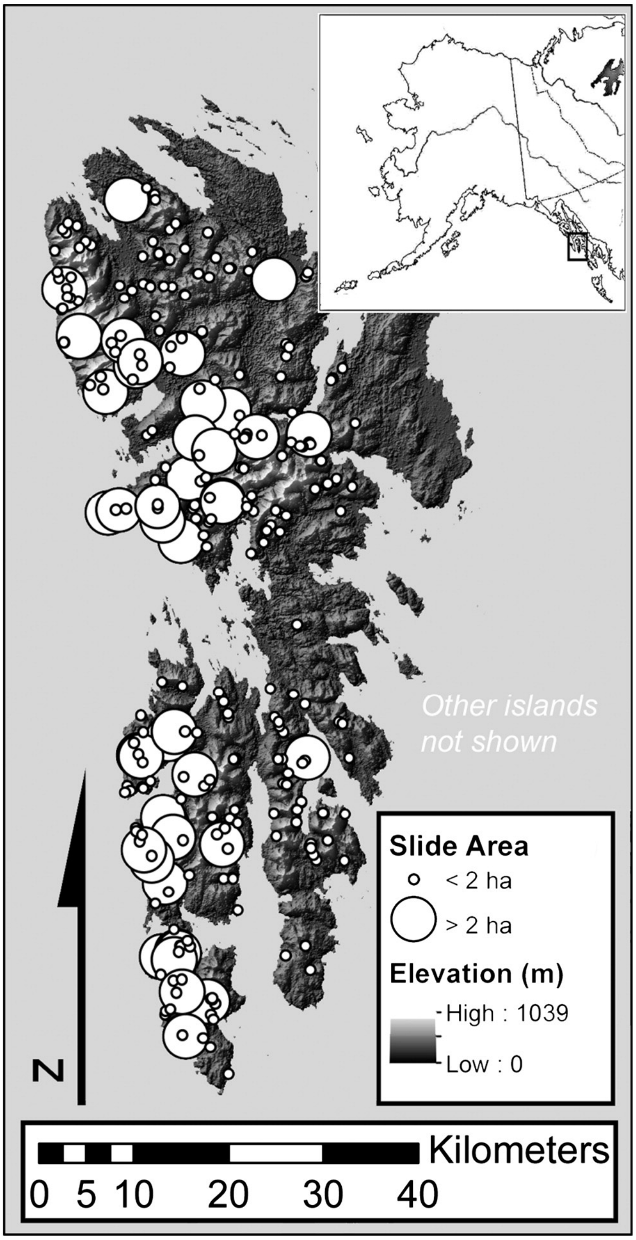

Fig. 1. Elevation (m) and landslides (highlighted zones) on Kuiu Island, Alaska. Landslides distributed across the topographically complex areas of the island, especially in the extreme north and south. Only natural slides are chosen, see Section 2 for selection procedure. Highlighted areas are larger than actual slides for visibility. Coordinates are UTM zone 8.

Table 1
Topographic statistics for the initiation and end points of natural landslides ($n = 295$) observed in forests on Kuiu Island (for units see Table 2).

Variable	Location	Mean (SD)	Median
Slope	Start	32.1 (10.1)	32.9
	Stop	23.8 (10.3)	23.1
TRASP	Start	82.5 (48.7)	79.3
	Stop	82.8 (45.8)	78.6
Terrain position index	Start	−0.3 (4.1)	−0.5
	Stop	−1.4 (3.9)	−1.6
Topographic index	Start	6.0 (1.23)	5.9
	Stop	8.1 (3.1)	7.2
Contributing area ($\log_{10}$)	Start	3.9 (0.5)	3.9
	Stop	4.3 (0.7)	4.2

2.1. Model construction

These slide locations represent locations that are susceptible to landslides. However, while landslides may not have been observed in other locations, that is not necessarily because landslides are impossible at that spot. Many areas where no slides are observed may still be likely places for landslides at some point in the future. This situation is true when considering initiation points for many disturbances (i.e., fire ignition points) and presents difficulties in modeling disturbance susceptibility and overall regimes because true absences (e.g., areas where disturbance initiation is impossible) are often unknown. Thus disturbance initiation data sets represent presence-only data, a common issue in species distribution modeling (Franklin, 2010). For this study, a generalized linear model (GLM; binomial response distribution, logit link) was used, following Bar Massada et al. (2013) who had success using GLMs with artificial absence points (randomly placed locations within the landscape) in predicting initiation points for wildfires, a similar problem of presence-only disturbance initiation points. This model form is one of the most commonly used methods in landslide susceptibility modeling (for a review of landslide susceptibility models, see Korup and Stolle, 2014). The output is the likelihood of being classified as a location similar to those points where landslides were observed, essentially the susceptibility (or suitability) of a location for landslide initiation. For artificial absences, 15,000 random background points were placed in the study extent; only those points in forested areas and with slopes, elevations, and precipitation totals within the range of observed landslides were retained (Table 2, final total $n = 4236$). The purpose of this limitation was to retain background points similar to presence points for rigorous analysis. An alternate approach would be to use initiation densities, a continuous response (e.g., slides/ha), to avoid the difficulty associated with presence-only data (Franklin, 2010). However, given the extreme topography of the region and the broad scale, a continuous response function is not feasible, as any spatial scale large enough to provide a useful variety of densities would overwhelm the signal from slope, aspect, and other topographic variables that are known to be important.

2.2. Coefficients

At each point (presence or background), coefficients were extracted for use in the GLM framework. Continuous variables were checked for normality prior to analysis and log transformed as necessary. Variables likely to be significant based on plot-level research were considered: slope, aspect, precipitation, contributing area, terrain position index (TPI), topographic index (ATB), hydric soils, the presence of YCD, and wind disturbance exposure (Table 2); all analyses were conducted at a 30 m pixel size. The topographically derived variables were taken or created from ASTER GDEM 2 data (LP DAAC, 2011; vertical accuracy 17 m at 95% confidence interval). The ASTER DEM had sinks filled via the TOPMODEL package (Buytaert, 2011) prior to processing. Contributing area ($\log_{10}$ transformed), ATB, and TPI were derived from the TOPMODEL package. Contributing area, the area upslope of a given point is a measure of potential amounts of hydrologic runoff. ATB is given as

$$ATB = (\ln CA)/(\tan G) \quad (2)$$

where CA is contributing area, and $\tan G$ is the slope gradient (Moore et al., 1991). The ATB is strongly related to soil moisture because, as catchment area increases and slope decreases, there is more potential for water accumulation at a given location. The TPI is the elevation at a pixel minus the mean of the eight surrounding pixels. The TPI is zero for flat ground, negative for hollows, and positive for points and represents fine-scale topography (Buytaert, 2011). Slope and aspect were calculated via the Raster package in R (Hijmans, 2013). To

Table 2
Variables, resolution, units, and ranges of spatial data sets used in creation of the GLM and as applied to the entire study area (total landscape).

Variable	Unit	Data Resolution original | final	Range (GLM model points)	Range (total landscape)
Precipitation	mm	771 m|30 m (nearest neighbor resampling)	2113–4916[a]	1561–5234
Contributing area (log10)[b]	m^2	30 m|30 m	2.95–6.87	0–1.9 × 10^7
Slope[b]	Degree	30 m|30 m	8–54[a]	0–79.8
Aspect (TRASP)	Degree, transformed [a]	30 m|30 m	0–180	0–180
Terrain position index (TPI)[b]	Relative meter	30 m|30 m	−17.2–23.6	−148–151
Topographic index (ATB)[b]	m^2/gradient	30 m|30 m	0–19.5	0–22.7
Hydric soils[b]	Presence/absence	30 m|30 m	0/1 (binary)	0/1 (binary)
Yellow cedar decline	Presence/absence	Polygon|30 m	0/1 (binary)	0/1 (binary)
Wind exposure[b]	NA	30 m|30 m	1–9	1–9

[a] See methods section.
[b] Indicates variable was significant in final model.

avoid circularity, aspect (in degrees) was transformed to TRASP (transformed aspect) as

$$TRASP = |aspect - 180| \quad (3)$$

which results in values of 180 for north and 0 for south.

Mean annual precipitation maps were provided by the Scenarios Network for Alaska & Arctic Planning (SNAP, 2013). Data is provided as annual means at a decadal timestep from 1910 to 2009, estimated via GCM's from observed climate (1971–2000), using the delta method of PRISM (prism.oregonstate.edu), downscaled to a 771 m resolution (data product: CRU TS 3.1.01). The mean annual precipitation was calculated for each pixel, downscaled to the resolution of analysis (30 m) via nearest neighbor assignment, and used in the model.

The USFS has mapped the location of YCD-affected areas (USFS, 2013; data available at: seakgis.alaska.edu) via low altitude flights and sketch mappers at a scale of 1:250,000. Maps show past decline and new decline as of the previous year. Because standing dead cedar may last for 80+ years and much of the observed decline areas occurred at unknown times prior to the initiation of the yearly survey, YCD presence was incorporated as a binary variable (presence/absence). This USFS map was converted to 30 m raster via nearest neighbor assignment. Hydric soils and cover type (forested/nonforested) have also been identified by USFS photointerpretation (available at: seakgis.alaska.edu). The maps were converted to raster layers at 30 m resolution via nearest neighbor assignment.

Exposure to wind disturbance was calculated similar to the methods in Kramer et al. (2001), based on work by Boose et al. (1994). Wind is modeled as a directional flow with elasticity in the vertical direction. The wind is allowed to inflect downward at a given angle after passing any barrier (e.g., a ridgetop). This inflection angle therefore influences the amount of landscape sheltered by topography from wind disturbance; high inflection angles result in less-sheltered areas. Boose et al. (1994) found that inflection angles of 6° well matched damage associated with hurricanes in temperate forests in New England. The Kramer et al. (2001) exposure index, tested and validated for Kuiu Island, used multiple inflection angles from 1° to 14° in 2° increments, for an index from 1 to 9 with 9 being the highest exposure level. Exposure to major windstorms is a function of southerly exposure, as major storms come from the south, southeast, and southwest, primarily during winter months (Harris, 1999; Kramer et al., 2001). The exposure index was calculated for winds coming from those directions and the mean recorded for the entire landscape.

All continuous variables were checked for significant spatial autocorrelation using Mantel tests with 10,000 permutations (Sokal, 1979). There were no significant spatial relationships ($p > 0.05$) observed except for precipitation, which was not significant in the final model (see Results) and thus ignored. All maps are available in Appendix 1.

2.3. Model evaluation

Initially, all variables were included in the GLM; the best combination was selected by stepwise Akaike information criterion (AIC) comparisons. The AIC is a model selection method that identifies the combination of variables that produce the most parsimonious model while still retaining a good fit to the data (Akaike, 1974); the model with the lowest AIC score is considered the best. Variables were successively removed based on the smallest decrease in AIC; selection stopped when the marginal AIC reduction was <3. This process was also followed for a no-wind null model consisting of the same potential variables except the wind exposure component. Following stepwise AIC model reduction, the final models (wind and no wind) were compared via the likelihood ratio test.

Accuracy and stability of the best model were assessed via bootstrapped receiver operating characteristic (ROC) analysis. Receiver operating characteristic analyses quantify the relative rate of classifying positives and negatives (in this case slide or nonslide points) correctly based on the model output and are frequently used to estimate the accuracy of classifier models (Fielding and Bell, 1997); in this case, the ROC analysis determines accuracy in predicting slide or nonslide locations. One thousand populations were pulled from the presence and background data points; each population was randomly selected with replacement (total population size = ½ full model population size). The cumulative ROC curve was generated, and a final mean area under the curve (AUC) for the entire set of bootstrapped runs was calculated using the ROCR package (Sing et al., 2005).

To identify any changes in the spatial pattern of landslide susceptibility (with consideration of wind), the model was run for the entire island, with and without wind exposure. A single difference map was then produced to identify the relative differences found when including wind exposure as a covariate in landslide probability modeling. Summary statistics for areas of the map that saw the greatest increase (top 5% of the difference distribution) were calculated as a means to explore where inclusion of the disturbance interaction was most important in model outcomes.

3. Results

Stepwise AIC model selection with the full suite of variables resulted in a parsimonious model consisting of slope, wind exposure, precipitation, TPI, ATB, contributing area, and hydric soil presence. Of those predictors, the GLM indicated that those factors, except precipitation, were all significant predictors of landslide start locations ($p < 0.05$; precipitation marginally significant: $p = 0.06$) as compared to background locations (Table 2). Susceptibility to landslide initiation increased with increasing wind exposure, slope, and contributing area (highly variable) and decreasing with ATB and TPI. Hydric soils (a binary variable) were also associated with higher probabilities of slide initiation. Yellow cedar decline presence/absence was not included in any significant model, although hydric soils were associated with higher slide suitability.

Partial dependency plots illustrate these relationships; plots were built by holding all coefficients but one at their median value and varying that one parameter along its entire range (Fig. 2). Slope has a strong influence on slide suitability when the other variables are held at their median, with the likelihood of slide suitability increasing rapidly. Wind had a small but positive effect at the median slope value (~20°), as did the other predictor variables. To explore overall sensitivity to slope, the same analysis was conducted while holding slope at 50° (~90th percentile) instead of at its median (Fig. 2). The effect of the wind–slide interaction is much stronger, as is the sensitivity to changes in all the other variables.

A comparison of the final GLM with and without the wind component (nested model comparison, likelihood ratio test) indicated that inclusion of the wind exposure parameter significantly reduced deviance ($p = 0.003$). The mean AUC (1000 bootstrapped runs) for the optimal model was 0.83 ($SD = 0.01$), indicating a good rate of discrimination. The curve has no abrupt changes, indicating no major thresholds associated with better or worse performance. Bootstrapped ROC curve results are available in Appendix 2.

The broad spatial pattern of landslide susceptibility was driven primarily by slope, as expected from previous research (e.g., Swanston, 1969; Johnson et al., 2000). Overall, the median change in landslide likelihood upon including wind was neither positive nor negative (mean = 0%, 1.3% SD), indicating that the predicted landscape-scale landslide rate (as a function of cumulative probability) does not differ (Fig. 3). Rather, inclusion of wind exposure refined the spatial likelihood, from an increase of 10% in some areas to a decrease of 8% in other areas. The difference map identified finer scale areas where probability did change when including wind exposure in the model (Table 3, Fig. 4). While exposed areas generally saw increases in their calculated susceptibility with the inclusion of wind, sheltered areas saw a decrease in susceptibility when wind was considered.

4. Discussion

The results illustrate the role that disturbance interactions, topography, and landscape play in the landslide regime of these forests. Within these forests, hillslope stability was influenced by topography (slope), topographic shape (local, TPI; coarse scale, ATB), upslope area (contributing area), soil condition (hydric soils), and the wind disturbance regime (as calculated through exposure).

Slope, soil saturation, and soil depth are frequently considered the major drivers of landslides (Swanston, 1969; Johnson et al., 2000), and that was confirmed here. For example, soil saturation on high slopes is associated with landslides resulting from a reduction in soil cohesion and an increase in pore pressure, reducing friction. Hydric soil presence, ATB, contributing area, and TPI are all proxy measures for that saturation process; they represent the physical processes of soil output (e.g., hydric soil having low water output), inputs (contributing area), and topographic concentration (at the local scale, 90×90 m for TPI; watershed scale, ATB), respectively. Precipitation amount has a lesser influence, selected as part of the stepwise AIC criteria but only marginally significant ($p = 0.06$) in the final GLM. Saturated soil, expected in high precipitation areas, is less stable (increased u, decreased σ); however, in this system with a minimum precipitation >1500 mm annually, total precipitation is likely rarely the limiting factor on sliding. In lower precipitation systems, it is likely that total amounts would be more important (see Section 4.3 for discussion on the limitations of annual precipitation).

4.1. Disturbance relationships

Yellow cedar decline was not associated with the best predictive models for landslide initiation, despite an observed relationship at local scales (Johnson and Wilcock, 2002). Yellow cedar decline is more prevalent in poorly drained, hydric soils where rooting depth decreases and fine roots are more exposed to mortality associated with cold events (Hennon et al., 2012). The relationship between YCD and landslide initiation could therefore be masked by the significant influence of hydric soils, which is a significant factor in landslide susceptibility at regional scales and in areas without yellow cedar. It could also result from the temporal lag associated with the YCD/landslide interaction—approximately 50 years, associated with the time required for substantial decay in the roots of dead trees (Johnson and Wilcock, 2002). While the USFS has been collecting data on new areas of YCD, it remains unclear as to when YCD areas on Kuiu began to die; if the decline was recent, then no interaction should be expected yet. Nonetheless, as the

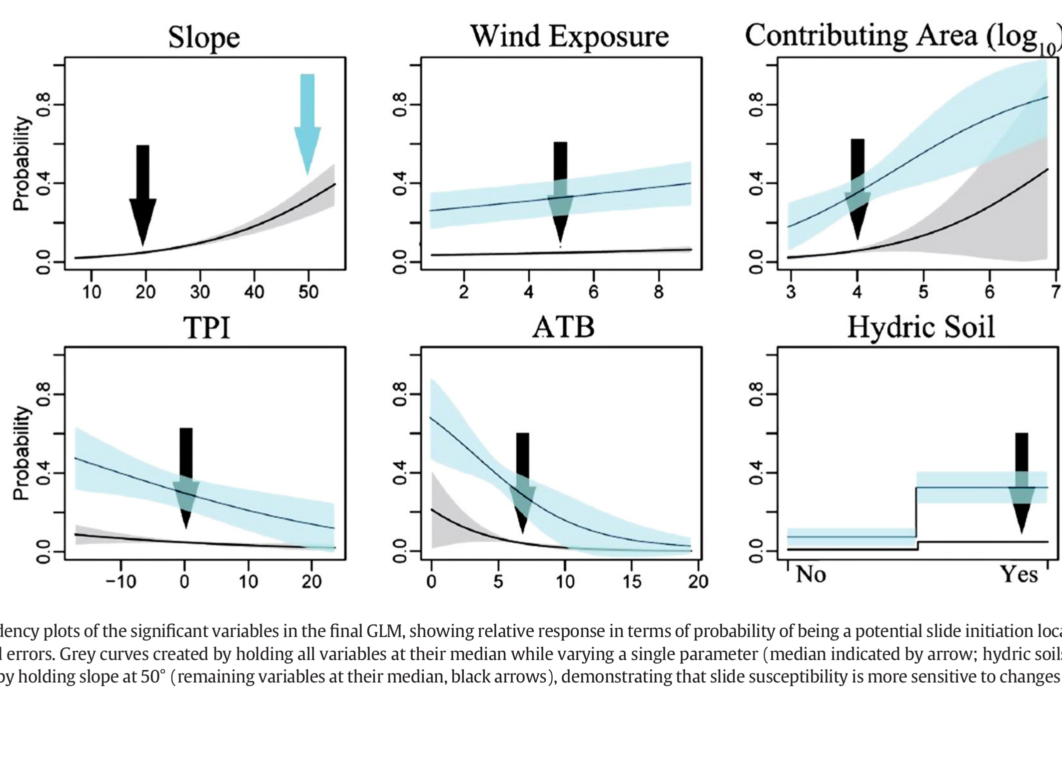

Fig. 2. Partial dependency plots of the significant variables in the final GLM, showing relative response in terms of probability of being a potential slide initiation location. Shaded area represents ±2 standard errors. Grey curves created by holding all variables at their median while varying a single parameter (median indicated by arrow; hydric soils is a binary response). Blue curves created by holding slope at 50° (remaining variables at their median, black arrows), demonstrating that slide susceptibility is more sensitive to changes in the other predictors at higher slopes.

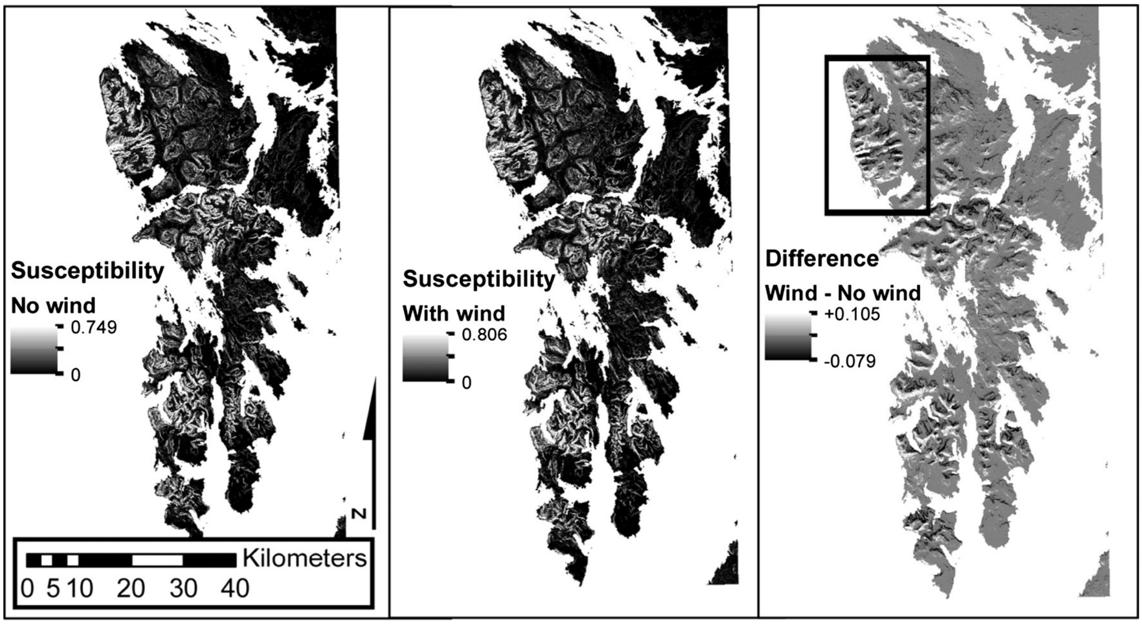

Fig. 3. Output maps for the final GLM models without wind (left), with wind (center), and the difference between the two (with–without; right). Average change in probability over the entire landscape was zero, as indicated by the general similarity at the island scale. However, spatial patterns changed, with some places having considerably higher probabilities (~14% increase) or lower (~17% decrease) when wind was included. Box indicates focal area for Fig. 4.

risk factors for YCD increase with climatic warming (Hennon et al., 2012), the observed relationship between YCD and landslides at the plot scale may emerge as important drivers of landscape-scale landslide patterns on Kuiu.

The wind exposure was a significant factor in landslide susceptibility. Higher wind exposure is positively associated with potential landslide initiation, confirming the expectation of Wu et al. (1979), Pawlik (2013), and other studies—although the effect was moderated by slope. At low slopes, wind was less important; but at high slopes (>40°), high wind exposure doubled susceptibility compared to low wind exposure (Fig. 2). Inclusion of wind exposure in the landslide suitability model shifted the spatial locations of high and low probability as well (Fig. 3). This is mainly seen by an increasing probability on exposed, south-facing steep slopes (Fig. 4), as hypothesized. This is likely a reflection of the role of vegetation in slope stabilization (*R* in Eq. (1)), which may be more significant on steeper slopes (Pawlik, 2013). The loss of vegetation and the corresponding increase in landslides is often seen in anthropogenic disturbances, such as logging or road-building (Sidle, 1992; Johnson et al., 2000). In southeast Alaska, hillslopes may be delicately balanced against the force of gravity (Swanston, 1997; Johnson et al., 2007); a relatively small reduction in root strength in combination with a downward force on trees associated with blowdown may have large effects on overall stability at high slopes—this is the case here (Fig. 2). All other factors equal, shallower slope angles may maintain integrity even through a destructive wind event, despite the loss of root support, due to friction between the soil and bedrock outweighing the effects of gravity on that soil body (Swanston, 1997), as indicated by the lowered sensitivity to wind exposure at lower slopes (Fig. 2). Sheltered areas saw a decrease in calculated landslide susceptibility. Root stabilization is likely important in these areas as well, and so the low exposure to wind disturbance results in a higher relative stability than would be expected based on topography alone (Pawlik, 2013).

Table 3
Mean (SD) of the continuous coefficients in spatial locations that saw the largest increase in landslide susceptibility (top 5%) when including wind.[a]

Variable	Value in sensitive areas
Slope	6.3 (7.4)
TRASP	35.4 (25.8)
ATB	5.8 (1.1)
TPI	−0.3 (4.6)
Precipitation	3982.3 (491.8)
Contributing area ($\log_{10}$)	3.9 (0.4)

[a] For example, areas that saw the greatest sensitivity to wind exposure were generally on steep slopes (mean = 36.3). For abbreviations/units see Table 2.

4.2. Application to other disturbances

This research has implications for disturbance interaction research. Broadly, the wind–landslide interaction did not change overall susceptibility (mean change = 0%). But at finer scales, relatively large changes in probability (−8%–+10%) were seen (Fig. 4). This results from the varying importance (across the landscape) of the factors described in Eq. (1). Essentially, other disturbances are only important when *R* is the limiting factor in slide susceptibility (i.e., locations where Eq. (1) is sensitive to changes in *R*). Similar to a limiting reagent in chemistry, disturbance interactions (focusing on those that act to increase/decrease disturbance likelihood) are likely only present when the limiting mechanistic factor is susceptible to some sort of interaction. For example, if wildfire ignition likelihood is primarily driven by anthropogenic presence (e.g., distance to roads; Bar Massada et al., 2013), then one should not expect to observe significant disturbance interactions via other mechanisms (for example, biomass desiccation through insect-driven vegetation mortality); however, there may be other interactions such as increased fire size if one does occur. Research on disturbance interactions should therefore identify the limiting mechanism driving their disturbance metric of interest (e.g., likelihood, extent) and examine how and where other disturbances might alter that particular mechanism—in this case, root stabilization.

4.3. Limitations

Southeast Alaska has relatively few spatial data sets despite being a center for endemic species, carbon storage, and natural resources (Orians and Schoen, 2013). Better data related to the spatial distribution of other coefficients, such as soil depth, would be useful in exploring the relative importance of the variables in Eq. (1). Seismically triggered

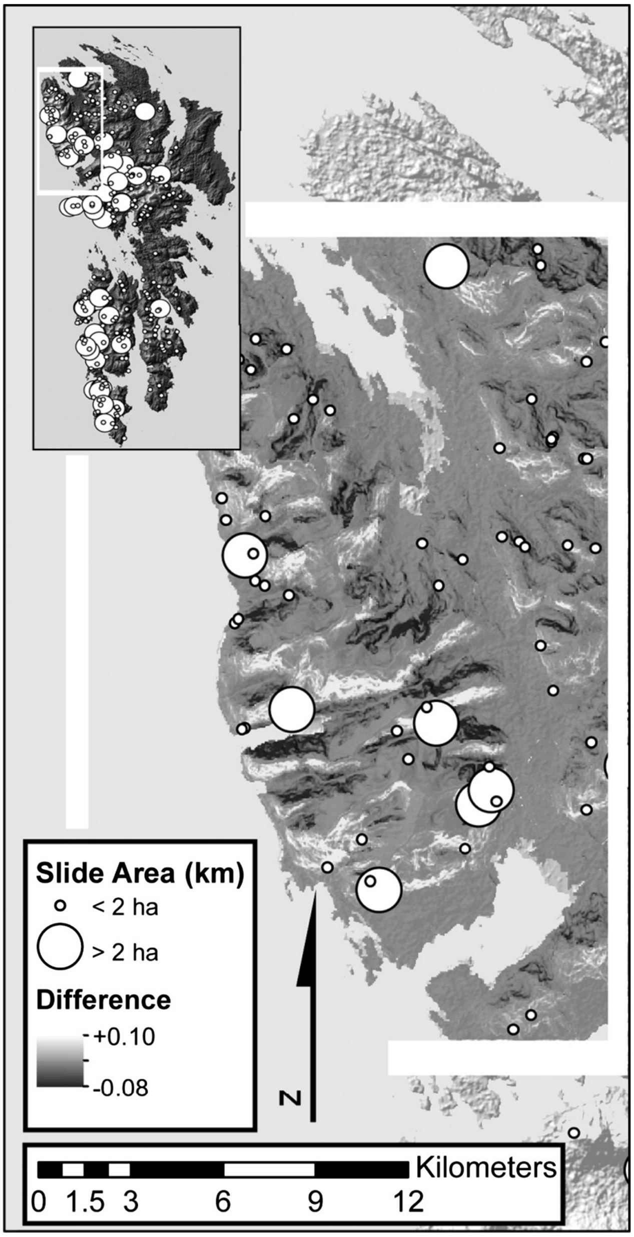

Fig. 4. A subset of Kuiu Island that highlights the change in suitability then including wind in the landslide model. Exposed areas (mostly southern aspects with no sheltering topography upwind) have higher predicted susceptibility, whereas sheltered southerly aspects or northerly aspects have lower predicted susceptibility. Inset same as Fig. 1 for reference.

landslides are a potential additional driver of events, however, as this would be seen as noise in the spatial data (as all exposures would experience any quakes); the significant relationship indicates that seismically driven events were not significant for this time period. Annual precipitation was only marginally important in these results. A better metric of precipitation would be potential rainfall in storm events, such as mm/h, as this would better describe the extreme events that often result in slides (Johnson et al., 2000). Maximum observed precipitation rates in the region have been estimated at 140 mm per 24-hour period; however, the spatial variation in those potential rates is not available at fine resolutions (Perica et al., 2012). Wind storms and high precipitation are often correlated, a potential complication; however, the fact that precipitation falls on wind-exposed and unexposed slopes alike indicates that wind is the dominate interaction here.

The data resolution used in this study, 30 m, represents the best spatial data available and balances tradeoffs between the wide extent studied and the fine-scale processes that influence landslide initiation. However, finer scale spatial processes (such as exposure or shelter from wind disturbance, small spatial patterns in drainage) may be missed because of the scale of investigation. Finally, the landslide data represents presence-only data (as does the majority of disturbance initiation data; e.g., Bar Massada et al., 2013). This presents methodological and statistical difficulties because there are no nonslide points, as it is unclear if a point is truly a nonslide location or simply a place where a landslide has yet to be observed. Randomized background points are used. This reduces the statistical power of the study as they could be in truly slide-susceptible areas. However, multiple lines of evidence support the conclusions: the significance of the wind exposure coefficient in the GLM, the significant improvement of the model over a null comparison via the likelihood ratio test, and the good AUC scores. Taken together, the conclusion that the wind regime is a significant driver of the spatial landslide regime seems reasonable.

5. Conclusion

There are significant interactions between the wind disturbance regime (as modeled using exposure) and landslide initiation locations. These interactions are subtle, not altering calculated susceptibility overall, but rather refining the spatial distribution of landslide susceptibility (increasing in some areas, decreasing in others). Areas with steeper slopes and on southerly aspects were associated with this interactive effect; the mechanism likely being a reduction in root strength as a result of tree mortality. Yellow cedar decline—associated with landslides in single-event, plot-scale studies—was not significantly associated with landslide initiation at this coarser scale of investigation. This could result from confounding variables (hydric soils) or a temporal effect associated with time since YCD onset, in which case its influence may increase in the future. This highlights the need to investigate disturbance interactions at multiple scales—as while interactions may cause interesting effects for individual events, they may be less significant at large spatial extents or for entire regimes. Awareness of the potential for these interactions is important, as changing climate and changing disturbance drivers may increase (or decrease) the relative importance of those individual and compound events.

Acknowledgments

This study received support from Alaska EPSCoR NSF award #OIA-1208927 and the State of Alaska. Thank you to Dennis Landwher, soil scientist with the USDA Forest Service, for advice during the preparation stage, and Bill Haneberg, two anonymous reviewers, and the editor for their helpful comments which greatly improved the manuscript.

Appendix A. Supplementary data

Supplementary data to this article can be found online at http://dx.doi.org/10.1016/j.geomorph.2014.10.014.

References

Akaike, H., 1974. A new look at the statistical model identification. Autom. Control. 19 (6), 716–723.

Alaback, P.B., 1991. Comparative ecology of temperate rainforests of the Americas along analogous climatic gradients. Rev. Chil. Hist. Nat. 64, 399–412.

Alaback, P.B., Nowacki, G., Saunders, S., 2013. Natural disturbance patterns in the temperate rainforests of southeast Alaska and adjacent British Columbia. In: Orians, G.H., Schoen, J.W. (Eds.), North Pacific Temperate Rainforests. University of Washington Press, Seattle, WA, pp. 73–88.

Ammann, M., Boll, A., Rickli, C., Speck, T., Holdenrieder, O., 2009. Significance of tree root decomposition for shallow landslides. For. Snow Landsc. Res. 82 (1), 79–94.

Bar Massada, A., Syphard, A.D., Stewart, S.I., Radeloff, V.C., 2013. Wildfire ignition-distribution modelling: a comparative study in the Huron-Manistee National Forest, Michigan, USA. Int. J. Wildland Fire 22 (2), 174–183.

Boose, E.R., Foster, D.R., Fluet, M., 1994. Hurricane impacts to tropical and temperate forest landscapes. Ecol. Monogr. 64 (4), 369–400.
Buma, B., 2014. Nutrient responses to ecosystem disturbances from annual to multimillennial timescales. New Phytol. 1, 13–15.
Buma, B., Wessman, C.A., 2011. Disturbance interactions can impact resilience mechanisms of forests. Ecosphere 2 (5) (art64).
Buma, B., Brown, C., Donato, D., Fontaine, J., Johnstone, J., 2013. The impacts of changing disturbance regimes on serotinous plant populations and communities. Bioscience 63 (11), 866–876.
Buytaert, W., 2011. Topmodel: implementation of the hydrological model TOPMODEL in R. R package version 0.7.2–2. http://CRAN.R-project.org/package=topmodel.
R Core Team, 2013. R: A language and environment for statistical computing. R Foundation for Statistical Computing, Vienna, Austria. URL http://www.R-project.org/.
Dale, V.H., Joyce, L.A., McNulty, S., Neilson, R.P., Ayers, M.P., Flannigan, M.D., Hanson, P.J., Irland, L.C., Lugo, A.E., Peterson, C.J., Simberloff, D., Swanson, F.J., Stocks, B.J., Wotton, B.M., 2001. Climate change and forest disturbances. Bioscience 51 (9), 723–734.
DeGayner, E.J., Kramer, M.G., Doerr, J.G., Robertsen, M.J., 2005. Windstorm disturbance effects on forest structure and black bear dens in southeast Alaska. Ecol. Appl. 15, 1306–1316.
DellaSala, D.A., Moola, F., Alaback, P.B., Paquet, P., Schoen, J., Noss, R., 2011. Temperate and boreal rainforests of the Pacific coast of North America. In: DellaSala, D.A. (Ed.), Temperate and Boreal Rainforests of the World: Ecology and Conservation. Island Press, Washington, DC, pp. 42–81.
Edburg, S.L., Hicke, J.A., Brooks, P.D., Pendall, E.G., Ewers, B.E., Norton, U., Gochis, D., Gutmann, E.D., Meddens, A.J.H., 2012. Cascading impacts of bark beetle-caused tree mortality on coupled biogeophysical and biogeochemical processes. Front. Ecol. Environ. 10, 416–424.
Fielding, A.H., Bell, J.F., 1997. A review of methods for the assessment of prediction errors in conservation presence/absence models. Environ. Conserv. 24 (1), 38–49.
Franklin, J., 2010. Mapping Species Distributions. Cambridge University Press, New York, NY (336 pp.).
Harris, A.S., 1999. Wind in the forests of southeast Alaska and guides for reducing damage. USDA Forest Service GTR PNW-244.
Hennon, P.E., D'Amore, D.V., Schaberg, P.G., Wittwer, D.T., Shanley, C.S., 2012. Shifting climate, altered niche, and a dynamic conservation strategy for yellow-cedar in the North Pacific Coastal Rainforest. Bioscience 62 (2), 147–158.
Hijmans, R.J., 2013. Raster: geographic data analysis and modeling. R package version 2. 1–66. http://CRAN.R-project.org/package=raster.
Hungr, O., Evans, S.G., Bovis, M.J., Hutchinson, J.N., 2001. A review of the classification of landslides of the flow type. Environ. Eng. Geosci. 7 (3), 221–238.
Hutchinson, O.K., LaBau, V.J., 1975. The forest ecosystem of southeast Alaska. 9: timber inventory, harvesting, marketing, and trends. USDA Forest Service GTR PNW-34.
Johnson, E.A., Cochrane, M.A., 2003. Disturbance regime interactions. In: Lovejoy, T., Hannah, L. (Eds.), Climate Change and Biodiversity: Synergistic ImpactsAdvances in Applied Biodiversity Science 4. Conservation International, Washington, DC, pp. 39–44.
Johnson, A.C., Wilcock, P., 2002. Association between cedar decline and hillslope stability in mountainous regions of southeast Alaska. Geomorphology 46 (1), 129–142.
Johnson, A.C., Swanston, D.N., McGee, K.E., 2000. Landslide initiation, runout, and deposition within clearcuts and old-growth forests of Alaska. JAWRA 36 (1), 17–30.
Johnson, A.C., Edwards, R.T., Erhardt, R., 2007. Groundwater response to forest harvest: implications for hillslope stability. JAWRA 43 (1), 134–147.
Kashian, D.M., Romme, W.H., Tinker, D.B., Turner, M.G., Ryan, M.G., 2006. Carbon storage on landscapes with stand-replacing fires. Bioscience 56 (7), 598–606.
Korup, O., Stolle, A., 2014. Landslide prediction from machine learning. Geol. Today 30 (1), 26–33.
Kramer, M.G., Hansen, A.J., Taper, M.L., Kissinger, E.J., 2001. Abiotic controls on long-term windthrow disturbance and temperate rain forest dynamics in southeast Alaska. Ecology 82 (10), 2749–2768.
Kulakowski, D., Veblen, T.T., 2007. Effect of prior disturbances on the extent and severity of wildfire in Colorado subalpine forests. Ecology 88, 759–769.
Kulakowski, D., Veblen, T.T., Bebi, P., 2003. Effects of fire and spruce beetle outbreak legacies on the disturbance regime of a subalpine forest in Colorado. J. Biogeogr. 30, 1445–1456.
LP DAAC (NASA Land Processes Distributed Active Archive Center), 2011. ASTER GDEM2. USGS/Earth Resources Observation and Science (EROS) Center, Sioux Falls, South Dakota, (Accessed October 2013).
McLauchlan, K.K., Higuera, P.E., Gavin, D.G., Perakis, S.S., Mack, M.M., Alexander, H., Battles, J., Biondi, F., Buma, B., Colombaroli, D., Enders, S.K., Engstrom, D.R., Hu, F.S., Marlon, J., Marshall, J., McGlone, M., Morris, J., Nave, L., Shuman, B.N., Smithwick, E.A.H., Urrego, D., Wardle, D., Williams, C., Williams, J.J., 2014. Reconstructing disturbances and their biogeochemical consequences over multiple timescales. Bioscience 64 (2), 105–116.
Mitchell, S.J., 2013. Wind as a natural disturbance agent in forests: a synthesis. Forestry 86 (2), 147–157.
Montgomery, D.R., Deitrich, W.E., 1994. A physically based model for the topographic control on shallow landsliding. Water Resour. Res. 30 (4), 1153–1171.
Moore, I.D., Grayson, R.B., Ladson, A.R., 1991. Digital terrain modelling: a review of hydrological, geomorphological, and biological applications. Hydrol. Process. 5, 3–30.
Nowaki, G.J., Kramer, M.G., 1998. The effects of wind disturbance on temperate rainforest structure and dynamics of Southeast Alaska. USDA Forest Service PNW-GTR-421.
Orians, G.H., Schoen, J.W. (Eds.), 2013. North Pacific Temperate Rainforests: Ecology and Conservation. University of Washington Press, Seattle, WA (416 pp.).
Paine, R.T., Tegner, M.J., Johnson, E.A., 1998. Compounded perturbations yield ecological surprises. Ecosystem 1 (6), 535–545.
Parker, K.R., Wiens, J.A., 2005. Assessing recovery following environmental accidents: environmental variation, ecological assumptions, and strategies. Ecol. Appl. 15, 2037–2051.
Pawlik, L., 2013. The role of trees in the geomorphic system of forested hillslopes — a review. Earth Sci. Rev. 126, 250–265.
Perica, S., et al., 2012. Precipitation-frequency atlas of the United States, Alaska. NOAA Atlas 14 Volume 7 Version 2.0. National Weather Service, Silver Spring, MD.
Sidle, R.C., 1992. A theoretical model of the effects of timber harvesting on slope stability. Water Resour. Res. 28 (7), 1897–1910.
Sidle, R.C., Pearce, A.J., O'Loughlin, C.L., 1985. Hillslope stability and land use. American Geophysical Union. Water Resources Monograph 11 (140 pp., Washington, D.C.).
Sing, T., Sander, O., Beerenwinkel, N., Lengauer, T., 2005. ROCR: visualizing classifier performance in R. Bioinformatics 21 (20), 3940–3941.
SNAP, 2013. Scenarios Network for Alaska and Arctic Planning. University of Alaska, (Retrieved 11/1/2013 from www.snap.uaf.edu).
Sokal, R.R., 1979. Testing statistical significance of geographic variation patterns. Syst. Zool. 28, 227–231.
Swanston, D.N., 1969. Mass wasting in coastal Alaska. USDA Forest Service Res. Pap. PNW-83.
Swanston, D.N., 1974. The forest ecosystem of southeast Alaska. 5: Soil mass movement. USDA Forest Service GTR PNW-17.
Swanston, D.N., 1997. Controlling stability characteristics of steep terrain with discussion of needed standardization for mass movement hazard indexing: a resource assessment. Assessments of Wildlife Viability, Old-growth Timber Volume Estimates, Forested Wetlands, and Slope Stability. USDA Forest Service GTR 392, pp. 44–58.
Terzaghi, K., 1943. Theoretical Soil Mechanics. John Wiley and Sons, Inc., New York, NY (528 pp.).
Turner, M.G., 2010. Disturbance and landscape dynamics in a changing world. Ecology 91, 2833–2849.
USFS, 2011. Tongass national forest landslides. Originator: USDA Forest Service. Point of Contact: Dennis Landwehr, 648 Mission Street, Ketchikan, AK 99901 (Available at: www.seakgis.alaska.edu).
USFS, 2013. Cumulative yellow-cedar decline. Originator: USDA Forest Service. Point of Contact: Dustin Wittwer, 11305 Glacier Highway, Juneau, AK 99801 (Available at: www.seakgis.alaska.edu).
Varnes, D.J., 1978. Slope movement types and processes. In: Schuster, R.L., Krizek, R.J. (Eds.), Landslides, Analysis and Control. Special Report 176. Transportation Research Board, Washington, D.C., pp. 11–33.
Veblen, T.T., Alaback, P.B., 1996. A comparative review of forest dynamics and disturbance in the temperate rainforests in North and South America. In: Lawford, R., Alaback, P.B., Fuentes, E.R. (Eds.), High Latitude Rain Forests of the West Coast of the Americas. Springer-Verlag, Berlin, pp. 173–213.
Veblen, T.T., Hadley, K.S., Nel, E.M., Kitzberger, T., Reid, M., Villabla, R., 1994. Disturbance regimes and disturbance interactions in a Rocky Mountain subalpine forest. J. Ecol. 82 (1), 125–135.
Walter, H., 1984. Vegetation of the Earth and Ecological Systems of the Geo-Biosphere. Springer-Verlag, Berlin (334 pp.).
White, P.S., 1979. Pattern, process, and natural disturbance in vegetation. Bot. Rev. 45 (3), 229–299.
Wiens, J.A., Parker, K.R., 1995. Analyzing the effects of accidental environmental impacts: approaches and assumptions. Ecol. Appl. 5, 1069–1083.
Wu, W., Sidle, R.C., 1995. A distributed slope stability model for steep forested basins. Water Resour. Res. 31 (8), 2097–2110.
Wu, T.H., McKinnell III, W.P., Swanston, D.N., 1979. Strength of tree roots and landslides on Prince of Wales Island, Alaska. Can. Geotech. J. 16 (1), 19–33.